

Geological and Mineralogical Investigations of Microgranites at the Southeastern Part of Wadi Baroud, North Eastern Desert, Egypt

Neveen S. Abed^{1*}, Mohamed Abdel Monsif⁴, Hesham M.H. Zakaly^{2,3} and Hamdy A. Awad^{4,5,1}

¹Geochemical Exploration Department, Nuclear Materials Authority, P.O. Box 530, El-Maadi, Cairo, Egypt.

² Department, Faculty of Science, Al-Azhar University, Assuit Branch, 71524 Assuit, Egypt.

³ Physics Department, Faculty of Science, Al-Azhar University, Assuit Branch, 71524 Egypt.

⁴ Southern Federal University, 344103, Rostov-on-Don, Zorge st., 40. Russia.

⁵ Geology Department, Faculty of Science, Al-Azhar University, Assuit Branch, 71524 Assuit, Egypt

Received: 1 Jan.2021, Revised: 26 Feb.2021, Accepted: 1 Mar.2021.

Published online: 1 May. 2021.

Abstract: Geological and mineralogical studies were conducted in the Southeastern part of Wadi Baroud in the Abu Hadeida region. This area contains older granites, younger gabbros, and younger granites, in addition to basic and acidic dikes. The younger granites include proper granites (lacking radioactivity) and anomalous microgranite offshoots. The microgranite offshoots are constituted by less altered, slightly radioactive portions and highly altered, radioactive mineralized rocks. Hematitization and silicification are the most common alteration features. The compound REEs were refilled with F in liquids, then re-deposited in dams and microscopic veins along weak levels, resulting in formation of the mineralized zone. The occurrence of radioelement-bearing minerals like xenotime, thorite, uranothorite, apatite, and allanite in the studied microgranite may lead to the metamictization of minerals and a loose structure. The reaction between metamict mineral and the hydrothermal fluid leads to an alteration in the chemical composition. The studied granites are enriched with many rare accessory minerals, such as the euxenite-polycrase series, the columbite-tantalite series, the samarskite group, uranium-thorium minerals, rare earth minerals (cerianite), Zircon and monazite.

Keywords: Wadi Baroud; microgranites; Eastern Desert; Egypt.

1 Introduction

The studied area is located in Egypt's Northeastern Desert, 20 km west of Safaga City. The area is easily accessible via the newly created part of Qena Safaga via an asphalt road that runs directly north of the area via W. Baroud Al Abyad. The latitudes border the area $26^{\circ} 42' 54''$ and $26^{\circ} 45' 36''$ N and the longitudes $33^{\circ} 44' 06''$ and $33^{\circ} 47' 42''$ E (Fig.1). The investigated rock units of the study area represent small part of the Arabian–Nubian Shield (ANS) that began at ~ 870 Ma and established at ~ 620 Ma ago, when convergence between East and West Gondwana fragments closed the Mozambique ocean along the East African – Antarctic Orogen (EAAO) [1, 2]. The ANS is represented by four main lithological components, juvenile arc supracrustured sequence, ophiolite, gneissic core complex and granitic intrusion [3]. According to field observations, the study area is lies along to largest shear zone (Qena-Safaga Shear Zone [4], so the areas affected by this shear zone to show metamorphic and non-metamorphic magmatic rocks are covering the study area.



Fig.1: Location Map of the studied areas.

Usually the resulting geological components are referred to as western arc of ANS (oceanic arc terrains of ANS)[5, 6, 7], this oceanic terrains above mentioned are collided and amalgamated with Afif and Tathlith terrains creating between 680 and 640 Ma to forming a new continental crustal block (proto-Arabian-Nubian Shield) (pANS) [6]. Moreover, the

*Corresponding author e-mail: nova848@yahoo.com

studied low-grade metamorphic rocks of oceanic terrains along the Qena-Safaga shear Zone represent a part of the older upper crust, that are thrust over the younger lower crust of high-grade metamorphic rocks gneisses and migmatites [8].

The area is characterized by rugged topography and high reliefs. Ras Abda cuts it, and Abu Hadedia wadis and wadi Baroud surround it in the North and wadi Um Taghir in the South. Few radiometric and mineralogical studies have been carried out in the Southern part of the Abu Hadeida area [9,10,11]. The present article's main purpose is to conduct geological, petrographical, and mineralogical investigations of South Eastern part of wadi Baroud area.

2 Experimental Methods

2.1 Sampling and Sample Preparation

Twenty samples have been collected from the different rock units and alteration zones in the studied area. The Selected have been investigated by the polarized microscope and also prepared and subjected to separation of heavy metals using bromoform solution (sp. Gr. 2.85 gm/cm³) followed by mineralogical investigation using binocular microscope, X-ray diffraction technique (XRD) and Environmental Scanning Electron Microscope technique (ESEM) in order to throw a light on the economic importance of these minerals.

2.2 Geological Setting

The examined area is mainly represented by basement rocks: these consist of older granites, younger gabbros, younger granites and microgranitic offshoots; in addition to basic and acidic dikes (**Fig.2**). This is the first timeradioactive mineralization has been detected in the studied granite in the Southeast of Wadi Baroud.

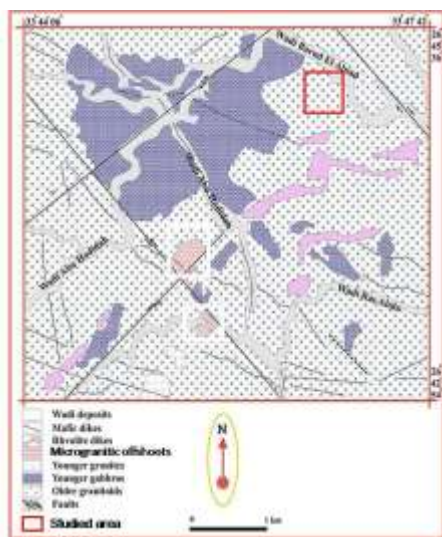


Fig.2: Geological map of Abu Hadeida area (Modified after Omran, 2014).

The younger granite is found in two phases, the first is proper (normal) granite with no mineralization and the second is mineralized granite which found as microgranite offshoots in the older granitoid (**Fig.3a**). The microgranite offshoots are represented by vertical walls (**Fig.3b**) with dimensions range from a few meters to tens of meters in length and less than a meter to a few meters in width. These microgranite offshoots are characterized by fine-to-medium grain and include various degrees of coloration, such as red, pink and reddish-pink, due to alteration processes. The zone of the microgranite off shoots has the highest level of radioactivity. Two types of altered granites were recorded in the studied area; the first is less altered microgranite while the second is highly altered and mineralized microgranite offshoots.

Several types of dikes have been found in the studied area. They differ in the mineralogical composition from acidic to basic that are cutting in older (**Fig.3c**) and younger granites, as shown in (**Fig.3d**). In some cases, basic dikes are the most recent rock unit; in contact with younger granite, they have a high radioactivity level. Quartz veins have also been recorded. They have lengths ranging from several meters to a few kilometres and widths ranging from several centimetres to a few meters, cutting through the older and younger granites (**Fig.3e**). Pegmatites have been found in many localities in various shapes (pocket and body) and unzoned forms. These are apart of fractures and joints and are found in both older and younger granites (**Fig.3f**) with various radioactivity levels (ranging from low to high).

On the other hand, the detailed sketch map of the studied area (**Fig.4**) show different rock units represented by older granite, younger granite and granite offshoots. Several alteration zones are found in the granite offshoots with clear mineralization, also two types of pegmatite are found in the studied area, the first is the mineralized pegmatite which related to the granite offshoots and the second one is the normal pegmatite related to the normal younger granite with no evidence of mineralization [12].

Generally, the studied granitic rocks have been affected by many hydrothermal alteration processes such as hematitization (**Fig.5a**), silicification and kaolinization associated with pegmatite pockets (**Fig.5b**) and chloritization. Manganese dendrites also affect the rocks to varying degrees of intensity (**Fig.5c**). Hematitization and silicification are the most common alteration features. Hematitization always exists in shear zones and is accompanied by visible uranium mineralization due to iron oxides' capacity to adsorb Uranium from its bearing solutions [13].

3 Results and Discussion

3.1 Petrography

The rocks of the studied area are classified microscopically into older granitoids (tonalite and granodiorite), younger granite (alkali feldspar), microgranite offshoots (alkali feldspar granite), and mafic dikes (dolerite and andesite).



Fig. 3:a) Younger granites intruded in the older granite, b) Microgranite offshoots in the older granite, c) Basic dike cut the older granite, d) Basic dike cut older and younger granite, e) Quartz vein cut in older granite and f) Pegmatite pocket in younger granite.

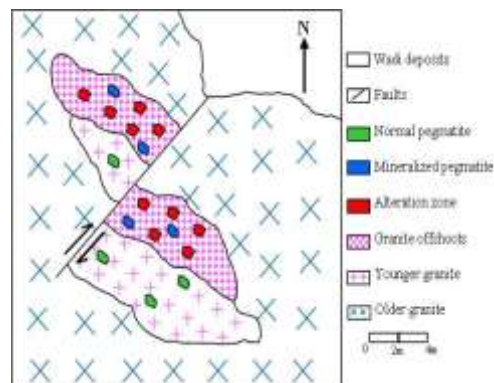


Fig.(4): Sketch map of the studied area.



Fig. 5:a) Hematitization in younger granite, b) Kaolinitization in younger granite and c) dendritic.

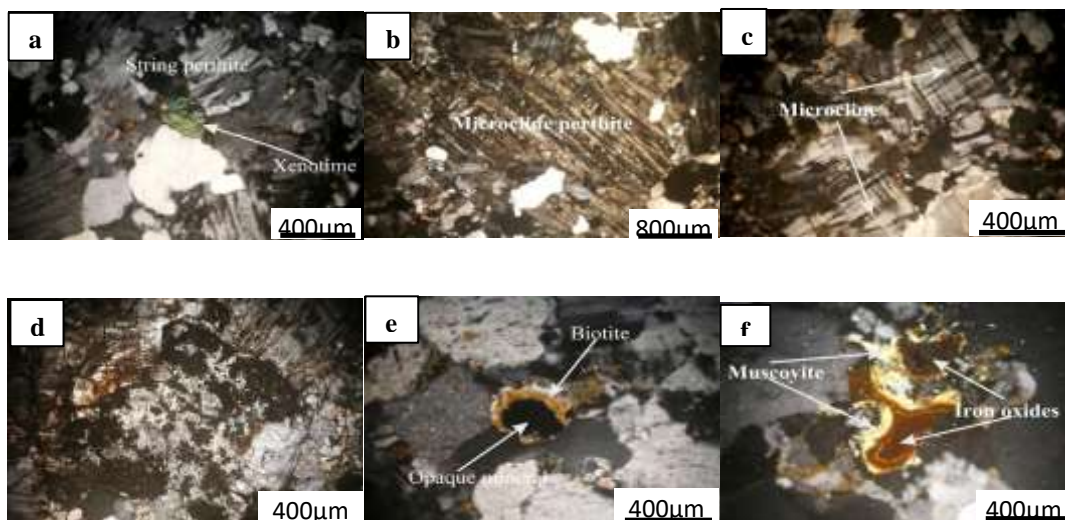


Fig. 6: a)Anhedralcrystals of string perthite, b)Anhedral crystals of microcline perthite, c)Anhedral crystals of microcline associating granules of quartz and perthite, d)Hematization andsericitization of perthite, e) Secondary biotite mantling opaque mineral and f) Muscovite enriched by iron oxides. (CN).

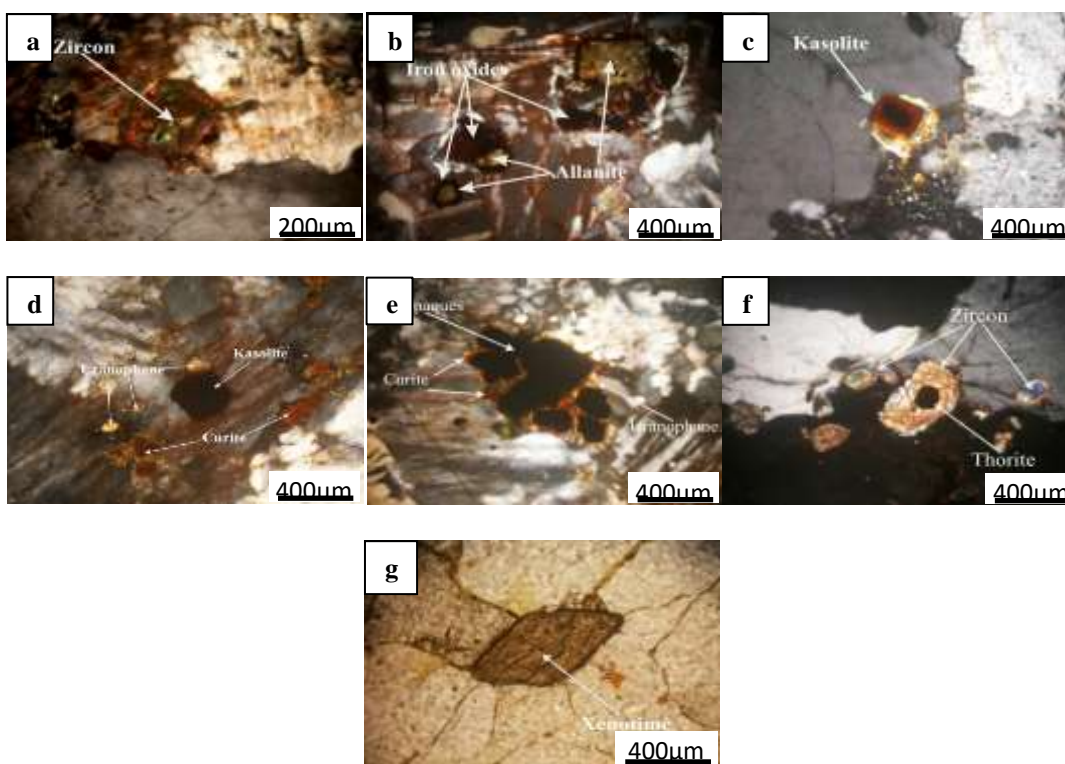


Fig. 7: a) A well-formed crystal of zoned zircon, b) Metamictizedallanite crystals coated by iron oxides, c) A well-formed crystal of kazolite with opaque inclusion, d) Uranophane, curite and kasolite, e) Uranophane, curite and opaques.CN, f) Metamict zircon with inclusion may be iron oxide (CN) and g) Bipyramidal crystal of xenotime surrounded with radial fractures. PI.

3.1.1 Microgranite Offshoots

The microgranite offshoots occur as fine-to-medium-grained alkali feldspar granite, which mainly consists of potash feldspars and quartz. They are characterized by an equigranular texture and are occasionally catalyzed, showing the quartz and potash feldspars' granulation. Potash feldspars are the main feldspars; plagioclase is wholly absent or occurs as an albite type that grows with the microcline to give perthite. Potash feldspars are present as anhedral crystals of string orthoclase perthite (**Fig.6a**) and microcline perthite (**Fig.6b**). Microclines are also present as anhedral crystals exhibiting a characteristic cross-hatched twinning (**Fig.6c**). Some potash feldspar crystals are hematitized and sericitized (**Fig.6d**). Mica minerals are rarely present, occurring as secondary biotite mantling the opaque minerals (**Fig.6e**) or as primary muscovite enriched with iron oxides (**Fig.6f**). Quartz represents about 25% to 30% of the rock.

3.1.2 Accessory Minerals

Zircon is the main accessory mineral: it has various forms and behaviors. It occurs as individual well-formed zoned crystals (**Fig.7a**) or as twinned crystals in perthite. Zircon also occurs as a cluster of fine crystals. Some of the zircon crystals are characterized by inclusions of opaque minerals or enclosing quartz. Other crystals are partially metamictized, pointing to the presence of radionuclides.

Allanite is the second accessory mineral present as a yellow crystal associating with iron oxides; it has its characteristic interference colors (second order) (**Fig.7b**). It can be partially metamictized, with the radionuclides causing its interference color to leak. Kasolite is also present as well-formed crystals characterized by their orange color: the opaque inclusions may be thorite (**Fig.7c**). Uranophane is the main uranium mineral present in the cavities: it is coated with secondary iron oxides, pointing to its epigenetic origin. It also occurs as clusters of radiating tiny yellow/greenish-yellow needles lining crevices (**Fig.7d**). Curite occurs as tiny orangish-red crystals associating with uranophane and opaques (**Fig.7e**).

Opaques occur in considerable amounts: the amounts increase significantly in mineralized zones (**Fig.7f**). The mineralized zones contain abundant accessory minerals, especially opaques, Zircon, allanite, curite, and fluorite. Opaques consist of iron oxides, pyrite, columbite, thorite, and uranohorite. The columbite, thorite, and uranohorite will be studied in detail later.

Silicification represents the main alteration feature in these rocks. It increases in highly mineralized zones, where it is entirely replaced by secondary silica. The silicified rock is mainly composed of quartz with an average grain size of 1.2 mm, digesting rock crystals (mostly plagioclase and quartz). The rock encloses an appreciable quantity of accessory minerals, such as aggregates of Zircon and Xenotime. Most of these accessories are metamictized, pointing to the presence of radioactive elements. Zircon is metamict and encloses opaque minerals like thorite, while xenotime crystals are

present as completely isotropic bipyramidal crystals (**Fig.7g**).

3.2 Mineralogical Investigations

The studied granites are enriched with many rare accessory minerals such as euxenite-polycrase series, the samarskite group, the columbite-tantalite series, Pyrochlore group, Betafite, uranopilite, accessory minerals (Zircon, and monazite), uranium-thorium minerals and rare earth minerals (cerianite).

3.2.1 Euxenite –polycrase series

These granites contain ABX_2O_8 euxenite group minerals and AB_2O_6 aeschynite group minerals as typical accessory minerals, including aeschynite, polycrase-(Y) and samarskite-(Y).

3.2.1.1 Euxenite $(Y, Ca, Ce, U, Th)(Ti, Ta, Nb)_2O_6$

Euxenite is the predominant REE-bearing mineral in the studied granite and occurs as prismatic or flattened black crystals, commonly metamict. Chemically, Euxenite is considered an oxide or titanite-columbite of the AB_2O_6 type. In the EDAX analyzed samples, $\sum Nb+Ta$ always exceeds Ti (**Fig.8a**). In these minerals, U varies between 14.44 to 41.32 % and Th from nil to 10.52 %, indicating their strongly radioactive nature and confirming their metamict state.

3.2.1.2 Aeschynite-(Y) $[(Y, Ca, Fe, Th)(Ti, Nb)_2(O, OH)_6]$

Aeschynite is a rare earth mineral, occurs as anhedral, black, and metamict disseminated crystals. The obtained EDAX analysis (**Fig.8b**) has illustrated the following elements in wt. %: Nb_2O_5 , 35.07; Ta, 2.63; Ti, 6.75; U, 14.45; Th, 7.00; Y, 9.74; Ca, 6.76; Fe, 2.87; Si, 3.71; Al, 2.48; K, 0.14; and a total REE of 8.38.

3.2.1.3 Uranopolycrase $(U, Y)(Ti, Nb, Ta)_2O_6$

Polycrase is the final member of a similar series of minerals: multiple oxides of Nb, Ta, Ti, and Y: it usually contains U, Th, and REE. It is thus called a rare earth oxide. Uranopolycrase is a very rare radioactive mineral that belongs to the polycrase group of minerals. Black radioactive uranopolycrase has been recorded in the studied granites. The EDAX analysis (**Fig.8c**) showed that the uranopolycrase in the samples contains U 22.28%, Nb 27.62%, Yb 0.81%, Er 0.72%, Th 8.30%, Ti 8.50%, and Ta 8.08%.

3.2.2 Samarskite Group

3.2.2.1 Samarskite (Y)

Samarskite is belonging to Nb-Ta mineral types that occur in pegmatite veins and granitic rocks and has the chemical form

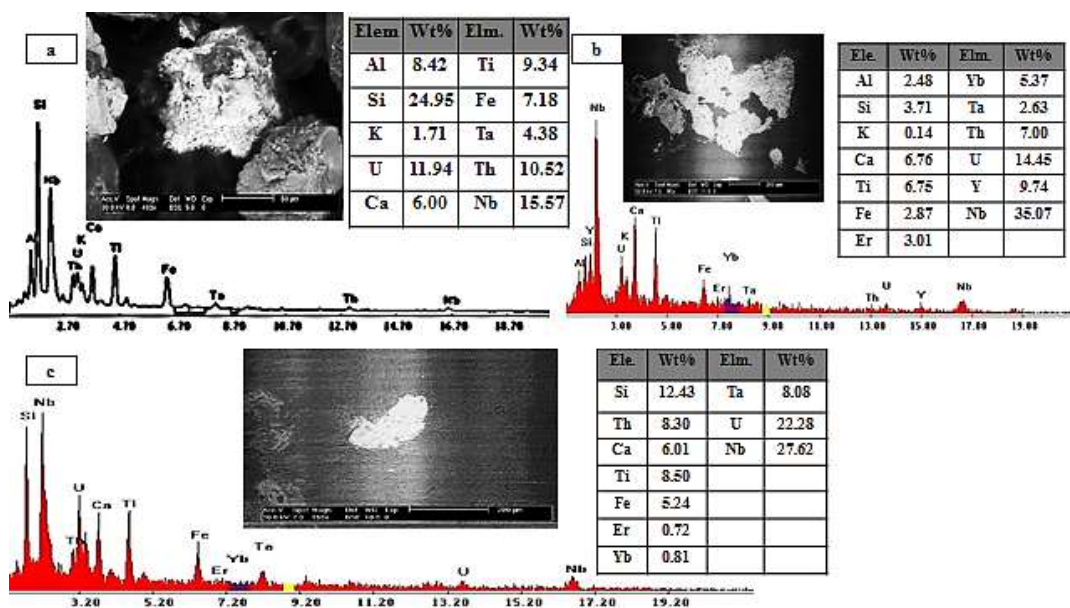


Fig. 8: EDX mineral analysis and BSE of: a- Euxenite, b- Aeschnite-(Y) and c- uranopolyrase.

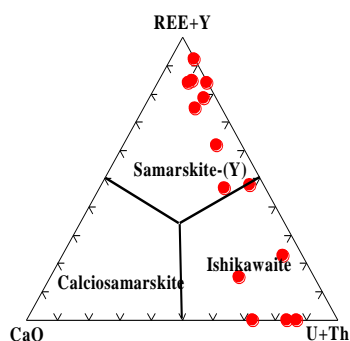


Fig. 9: Ternary diagram showing samarskite-group minerals after (14) in the studied area.

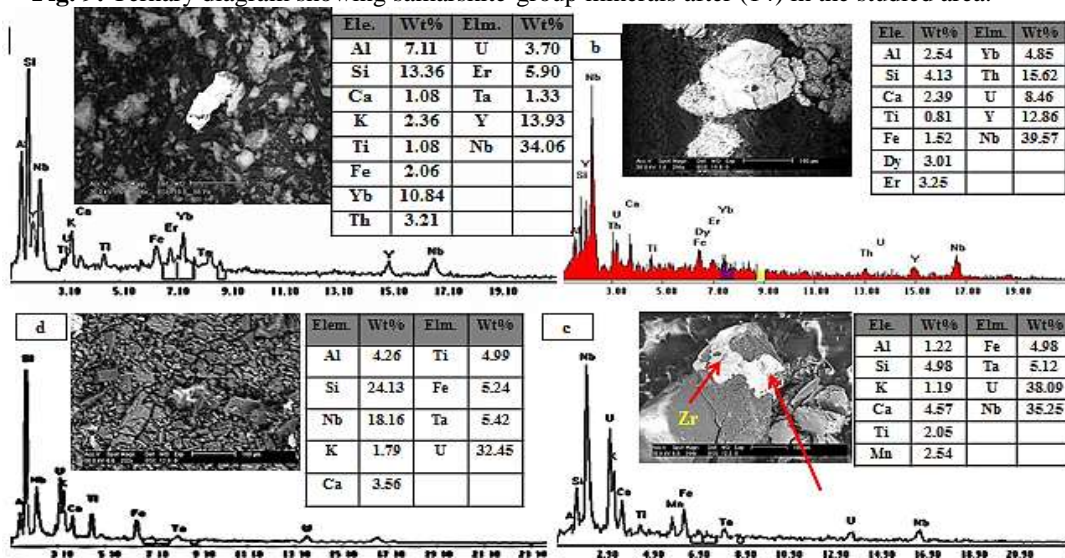


Fig. 10: EDX mineral analysis and BSE of: a, b- Samarskite, c and d- Ishikawite.

$ABnO_{2(m+n)}$, usually A include on Fe^{2+} , Ca, REE, Y, U, and Th; B are represented by Nb, Ta, and Ti. [14], they said the complete metamict state, the wide variety of cations, as well as the changes that take place in the site A, make their morphology relatively complex. Therefore, the authors divided the samarskite group into three mineral types. If REE + Y are dominant, this is called a (REE + Y) of samarskite and used as a suffix with predominant cations. If samarskite has high U + Th, this is called ishikawaite, otherwise known as calico samarskite if Ca is dominant.

[14] they concluded that ishikawaite and calico samarskite do not have light rare earth elements (LREE) while contain on heavy rare earth elements (HREE), associated with Y. In the recent time, samarskite-(Yb) is represented by a new types of the samarskite group [15], such as samarskite-Y. Otherwise, samarskite-Y is recognized by a mineral with Y + REE dominant at the A-site [16] as shown in (Fig.9).

The investigated samarskite grains are generally translucent, compact, metamict, a deep green colour, and massive, with a vitreous or resinous luster. The EDAX analysis ranges of the investigated samarskite grains (Fig.10) indicates that this mineral is enriched with Nb (23.11- 40.87%) and Y (6.6-13.93%). The contents of other REEs with radioelements are relatively high; namely, Er (0.00-5.57%), Dy (0.00-4.82%), Ce (0.00-3.11%), Nd (0.00-1.23%), La (0.00-1.23%), Sm (0.00-1.46%), Dy (0.00-4.82%), Yb (0.00-10.84%), U (3.7-13.56%), and Th (3.21-15.62%).

3.2.2.2 Ishikawaite

Varieties of samarskite (ishikawaite) have also been identified as inclusions in columbite. They occur as euhedral to subhedral minute crystals with blackish green or bright colors (Fig.10). The EDAX analysis confirmed the composition of ishikawaite: it contains mainly U (32.45-35.25%), Nb (18.16-35.25%), Ta (5.12-5.42%), and Fe (4.98-5.24%). EDAX analyses have been plotted on the standard diagram of [14], which appears the investigated grains of samarskite fall in the fields of Y- samarskite and ishikawaite (see fig.9).

3.2.3 Columbite-Tantalite Series

3.2.3.1 Columbite ($FeNb_2O_6$)

Minerals of the columbite-tantalite group are represented by a chemical formula AB_2O_6 , where the site of A contains Fe, Mn, and low contents of Mg and Na in addition to the valence of the triple ion. The B site contains Nb, Ta, and small contents of Ti and W. The isoivalent substitutions in columbite are $Fe \leftrightarrow Mn$ at the A site and $Nb \leftrightarrow Ta$ at the B site, with corresponding ferrocolumbite, manganocolumbite, ferrotantalite, manganotantalite end members [17,18]. The enrichment of columbite with U and Y is also recognized. Heinrich (1962) [19] indicated that U-bearing columbite is Ta-poor: increasing U content according to a decrease in crystallization temperature. Under a binuclear microscope, columbite grains are characterized by a deep green colour

with a metallic to submetallic luster. Uranium-rich columbite and ferrocolumbite were recognized in the studied granites, as registered by the EDAX analyses (Fig. 11).

3.2.3.2 Fergusonite ($YNbO_4$)

The fergusonite group comprises REE-bearing Nb and Ta oxides, many of which are metamict and have a weak's properties. Related to other (Y, REE, U, Th)-(Nb,Ta,Ti) oxides, fergusonite (ideal formula: $YNbO_4$) represents typically as an additional contents in granitic rocks [20] and pegmatites [21]. On the other hand, fergusonite and other Nb-Ta-Ti oxide minerals are mostly influenced by altering chemical processes [21,22]. The EDAX analyses of the examined fergusonite crystals (Fig.12) clarify that the mineral has high contents of niobium, yttrium, ytterbium and REE elements in addition to Uranium and thorium.

3.2.4 Pyrochlore

3.2.4.1 Plumbopyrochlore

Pyrochlore group minerals have a wide formula range in terms of the A- and B-site cation substitutions. This group is a fundamental group, as Nb-Ta-Ti oxides contain significant levels of U subgroups of U. niobium exceeds Ta in the Pyrochlore subgroup, while Ta Nb exceeds in the microlite subgroup. Both Pyrochlore and microlite subgroups contain $(Ta + Nb) > 2Ti$, while the betafite subgroup is characterized by $2Ti > Ta + Nb$. U substitutions in site A and metamict pyrochlore are common. Although nearly all these minerals contain some amounts of U, only two minerals from the Pyrochlore group contain U as a primary component: urano microlite and urano pyrochlore [23,24] (Fig.13c). The EDX mineral analysis and BSE of pyrochlore [25] has led to the A proposal for a new nomenclature for the perchlor subgroup based on the ions present at the A, B and Y sites. Scientists have deduced five groups based on the atomic ratios of B, Nb, Ta, Sb, Ti and W. atoms, and the recommended groups are Pyrochlore, microlite, romeite, betafite, and elsmoreite respectively.

3.2.4.2 Uranopyrochlore

Urano pyrochlore is characterized by subhedral/ anhedral crystals in columbite, has a size ranging from 5 to 10 μm (Figs.13a, b and d). The EPMA analyses of the crystals show that urano pyrochlore has major elements such as: Nb_2O_5 (35.28 %), Ta_2O_5 (20.03%), and UO_2 (14.84%). Otherwise, pyrochlore contains a little amount of Th, Y, and LREE.

In the investigated pyrochlore types, the average amount of Nb reached about 19.79 %, higher than the average content of Ta (0.88 %). The analyses reveal that the average of Nb and Ta level is 20.86 %, which is significantly higher than the average of 2Ti level (4.2 %). The examined pyrochlore types have high Uranium content at the site of A, with ranging from 23.62 to 41.32 %, with an average reach of

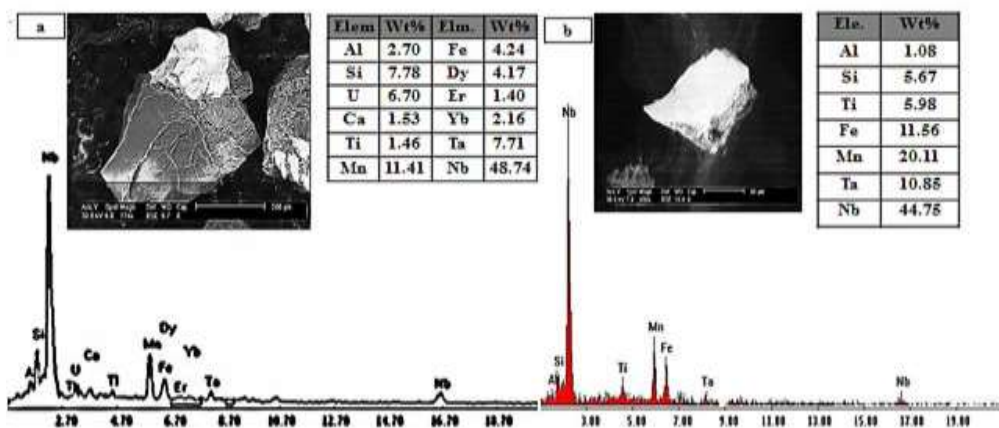


Fig. 11: EDX mineral analysis and BSE of a)columbite b)mn- columbite.

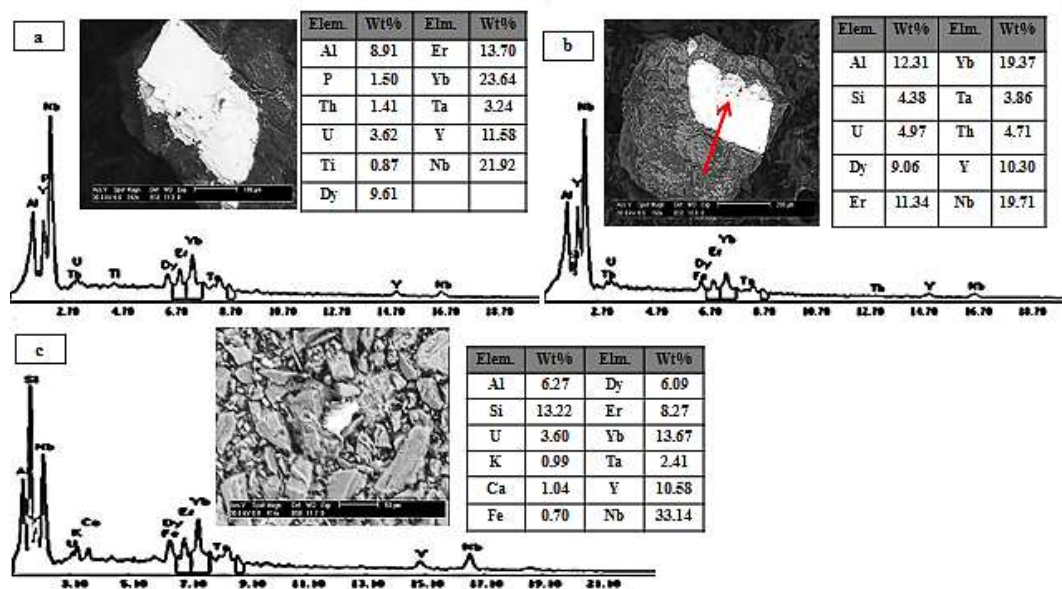


Fig. 12: EDX mineral analysis and BSE of fergusonite.

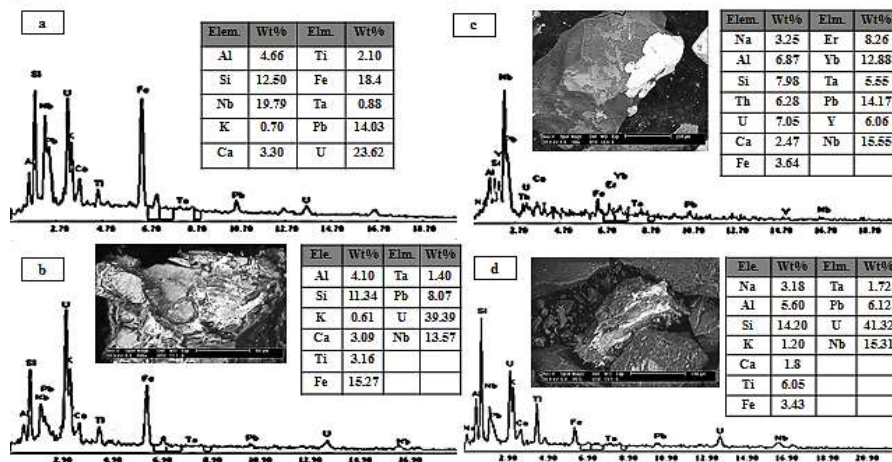


Fig. 13: EDX mineral analysis and BSE of: a,b, d- uranopyrochlore c- plumbopyrochlore.

about 32.47 %. Subhedral/ anhedral minute crystals represent pyrochlore in the studied granites. Our studies characterized pyrochlore species showed the compositional limits of urano pyrochlore and plumbo pyrochlore minerals species. Uranium and lead enrichment are indicated by the EDAX analyses (see **fig.13c**). Urano microlite $(U, Ca)_2(Ta, Nb)_2O_6(OH)$ was also identified by XRD analysis (**Fig.14**).

3.2.5 *Betafite* $[(U, Ca)(Nb, Ti)_2O_6]$

It is very rare: it recognized by as small anhedral grains in the microgranites of the studied area. The EDAX analysis of betafite (**Fig.15**) appears the presence of U and Th and in addition to Ti and REE.

The betafite was also determined by X-ray diffraction (XRD), (**Fig.16**). Nb is mainly substituted with Ti at the B-site in the studied area, which approach the composition of Betafite.

3.2.6 *Urano Pilite* $[(UO_2)_6(SO_4)O_2(OH)_6(H_2O)_6](H_2O)_8]$

This study has registered urano pilite (uranyl-sulfate mineral) for the first time in Egypt. It occurs especially in minute aggregates that consist of long prismatic crystals with a deep lemon yellow/pale greenish-yellow color. XRD only recognizes it due to its association with multiple phases of Nb-Ta mineralization (**Fig.17**).

3.2.7 *Accessory Minerals*

3.2.7.1 *Zircon*

According to microscope examination of zircon mineral, it occurs as euhedral prismatic and/or bipyramidal grains with different colors (pale yellow, reddish-brown, reddish-orange, and colorless): they are sometimes changed to opaque. The euhedral shape of zircon suggests its magmatic origin. Zircon grains are represented by multiple growths (**Fig.18**). This mineral was also identified by X-ray diffraction (**Fig. 19**).

Some of the studied zircon grains are metamictized and filled with pores, mainly distributed as black patchy domains containing other minerals (altered areas). Scanning electron microphotographs confirm that the examined zircon grains contain numerous black inclusions, such as thorite, uranothorite, and REE-bearing mineral (**Figs. 20, 21, and 22**).

3.2.7.2 *Uranium and Thorium Minerals*

3.2.7.2.1 *Thorite*

It is present as discontinuous brown/blackish-brown grains with size from less than 70 μm in diameter to 400 μm . Occasionally, it looks like Zircon due to its shape as small square prismatic crystals with pyramidal ends. The mineralogical studies for thorite indicate that the major elements are Th (52.82 wt %), Si (24.46 wt %), and U (8.09 wt %). Small

amounts of iron (3.03 wt%), calcium (1.07 wt%), and aluminium (6.7 wt%) have also been reported as alternatives (see **fig.20**). Sometimes, it is deposited as inclusions within dark, imperfect change regions in the zircon host's crystals. Thorite inclusions are small (less than ten μm).

3.2.7.2.2 *Uranothorite*

Uranothorite is characterized by pale to dark yellow-brown crystals that are typically translucent or opaque. It occurs as anhedral/ subhedral massive crystals with a granular form and distinctive glass or resinous shape and luster. According to the EDX analysis the uranothorite contains on major elements such as: Th (44.86 to 54.96 wt %), Si (19.88 to 23.60 wt %), and U (11.64 to 20.44 wt %). Minor amounts of Fe (1.88 to 5.68 wt. %), Ca (1.09 to 2.65 wt %), and Al (2.24 to 3.95 wt %) were also represented in uranothorite. The backscattered images showed that uranothorite is mostly included in Zircon (see **figs. 20, 21 and 22**).

3.2.8 *REE Minerals*

3.2.8.1 *Cerianite*

Rare earth minerals mainly occur in the fine-grain fraction (<1 mm) and are composed of various rare earth elements. These minerals are mainly enriched with Ce, La, Pr, Sm, and Nd, suggesting that they chiefly result from rare earth minerals enriched with thorite or uranothorite dissolution. Thorite ($ThSiO_4$) has a cerium composition with a significant solubility for Ce and Nd-rich components (ionic radii 1.09 Å, 1.08 Å, respectively, where Th has an ionic radius of 1.08 Å) [26]. Cerianite (Ce-oxide mineral) is found when Ce levels reach 39.09 wt. % and contain 4.30 wt. % Nd, in addition to 13.59 wt. % La (**Fig. 23a**). The enrichment of cerianite with La classifies it as the La-rich variety. Cerianite is a sensitive indicator of mineral formation conditions, as Ce is the only compatible REE that can occur not only in trivalent, but also in tetravalent form in natural conditions. Cerianite is formed only in strongly oxidizing conditions, mainly in alkaline solutions (fluids) [27, 28].

3.2.8.2 *Monazite*

Monazite grains are present as sub rounded to rounded grains, with transparent and vitreous luster. They are generally brownish red and reddish orange, mostly due to staining with iron oxides. Some grains are usually coated or emplaced in iron oxides. They are rare and increased in the finer grain size. Monazite grains were hand-picked and analyzed using the EDAX technique. The EDAX analyses reflect the chemical composition of monazite (**Fig. 23b**).

4 *Discussions*

The less altered microgranite has lower HFSE and REE content in comparison with the altered and mineralized microgranite from Abu Hadieda, as illustrated in Table 1

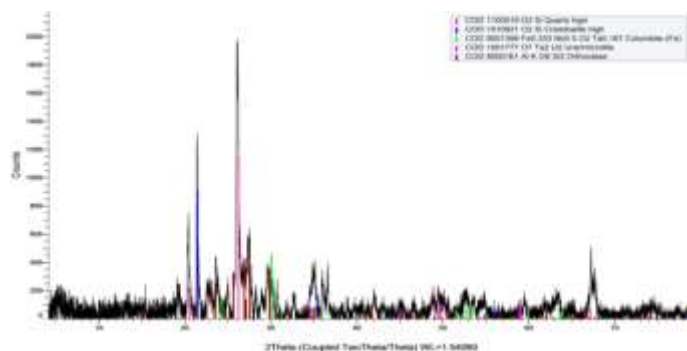


Fig. 14: X-ray diffraction pattern of uranomicrolite, columbite.

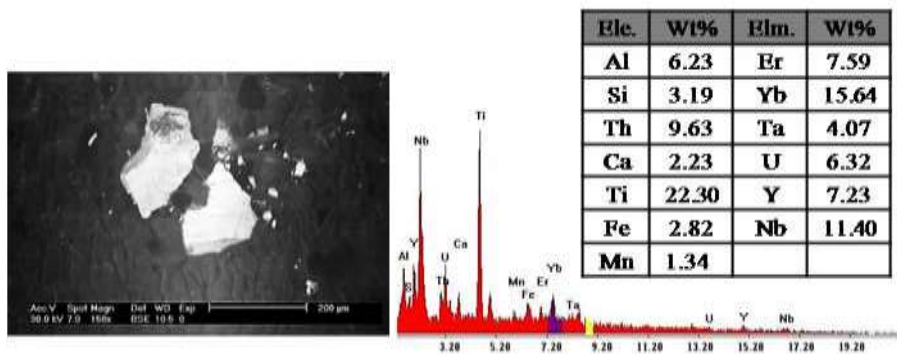


Fig. 15: EDX mineral analysis and BSE of betafite.

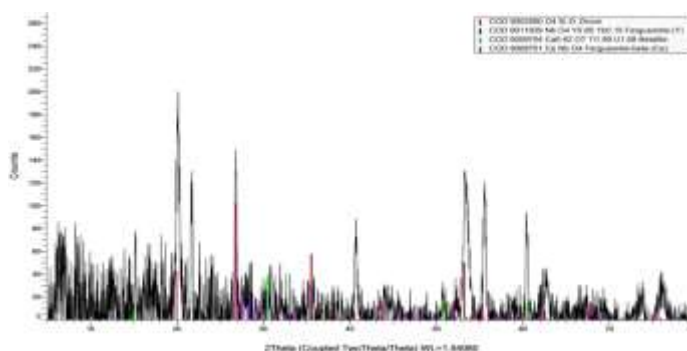


Fig. 16: X-ray diffraction pattern of zircon, fergusonite and betafite .

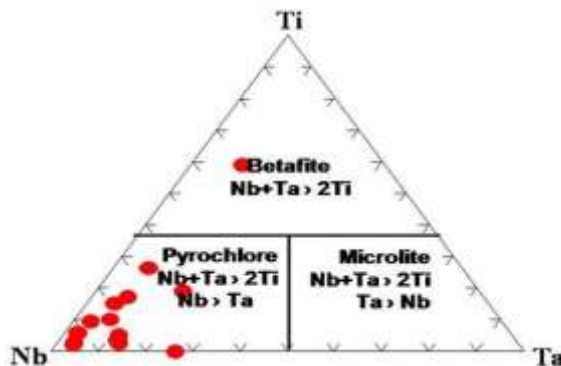


Fig. 17: Ternary diagram showing Pyrochlore-group minerals in the studied area.

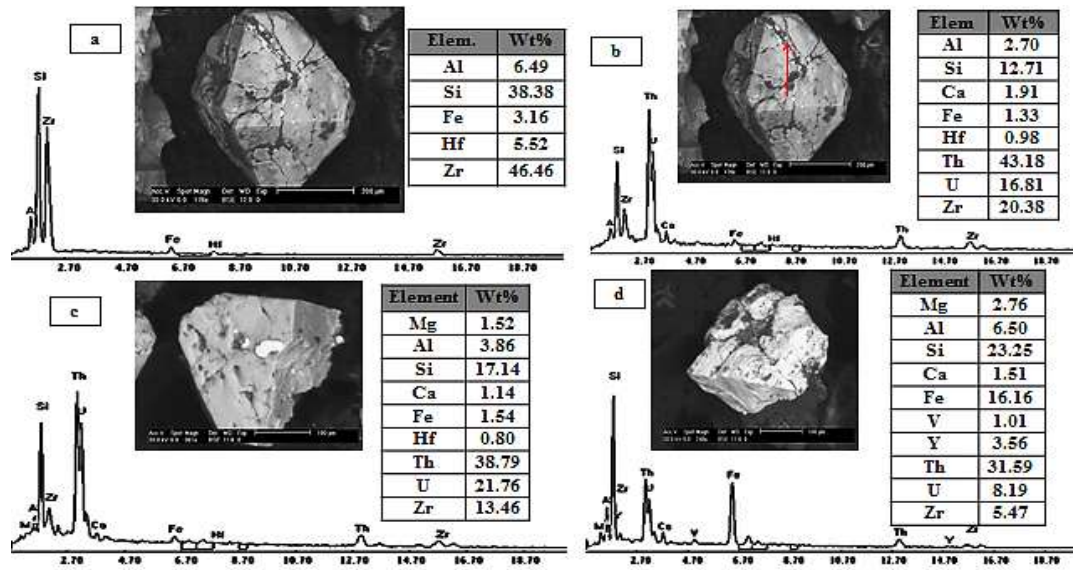


Fig. 18: a- BSE, binocular images and EDX analyses of metamict zircon. b- BSE, binocular images and EDX analyses of uranothorite as fissure filling in zircon. c- BSE, images and EDX analyses showing uranothorite as inclusion in zircon. d- BSE, binocular images and EDX analyses of thorite with V, Y, Zr.

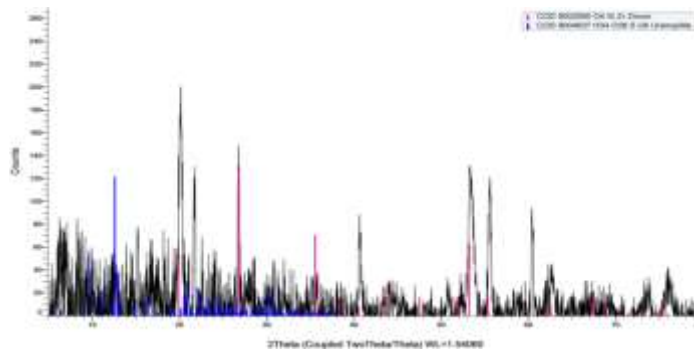


Fig. 19: X-ray diffraction pattern of uranopilite-zircon.

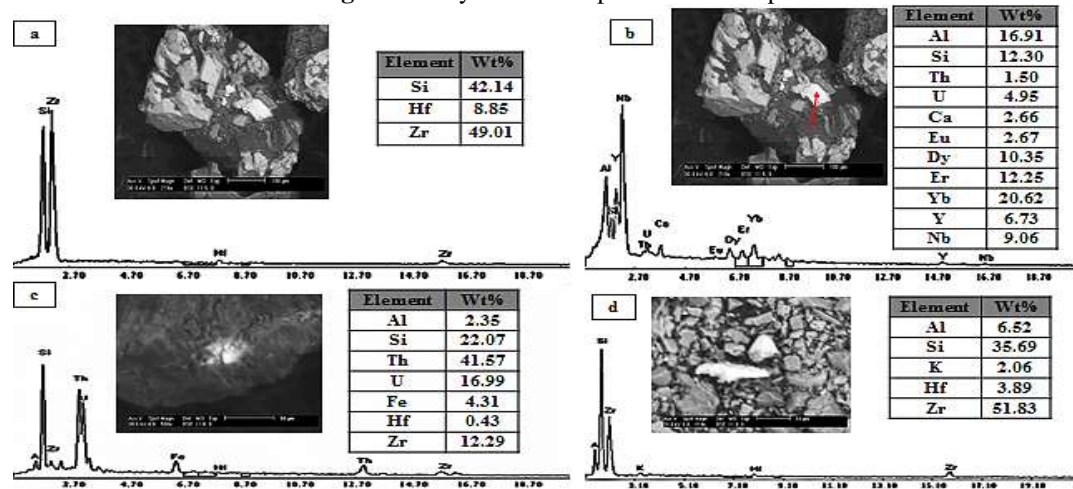


Fig. 20: a- BSE, binocular images and EDX analyses of zircon. b- BSE, images and EDX analyses of Nb, Y and REE and also uranothorite as inclusion in zircon. c- BSE, images and EDX analyses of uranothorite as inclusion in zircon. d- BSE, binocular images and EDX analyses of zircon.

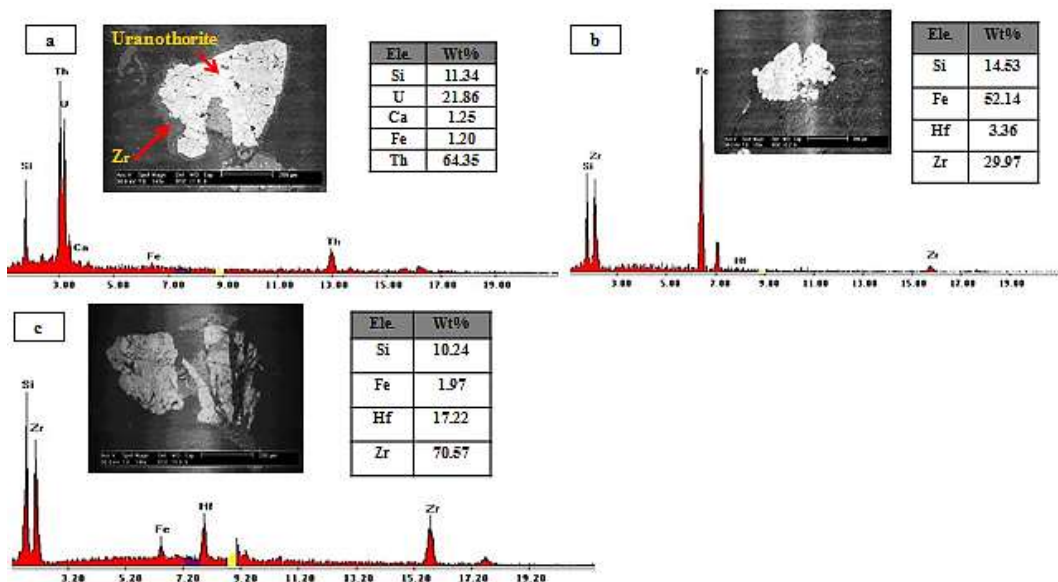


Fig. 21: BSE, binocular images and EDX analyses of: a- Uranothorite replace zircon, b- zircon with high Fe, c- zircon with high Hf.

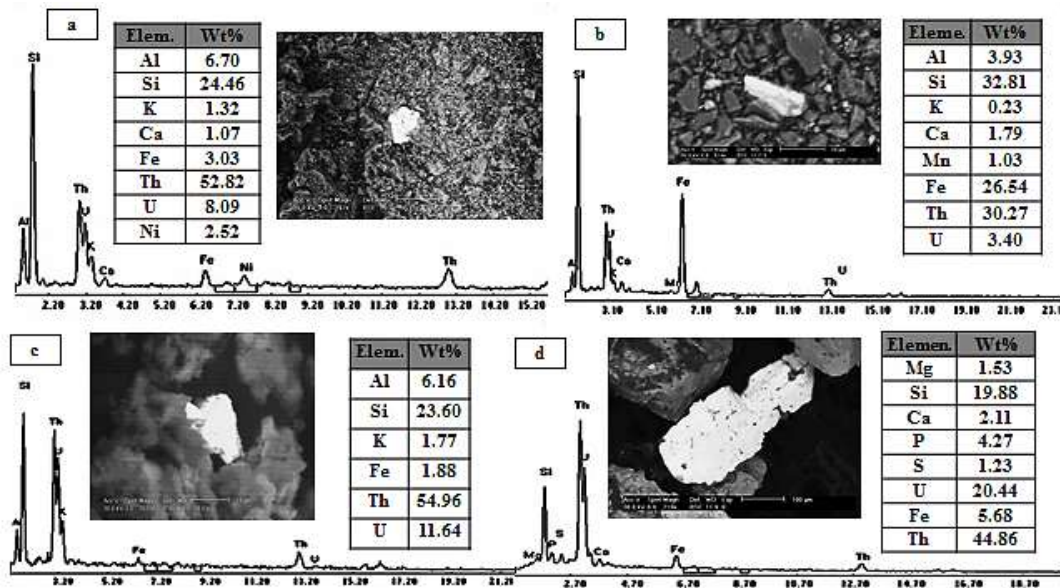


Fig. 22:a& b BSE images and EDX analyses of thorite minerals. c& d- BSE images and EDX analyses of uranothorite.

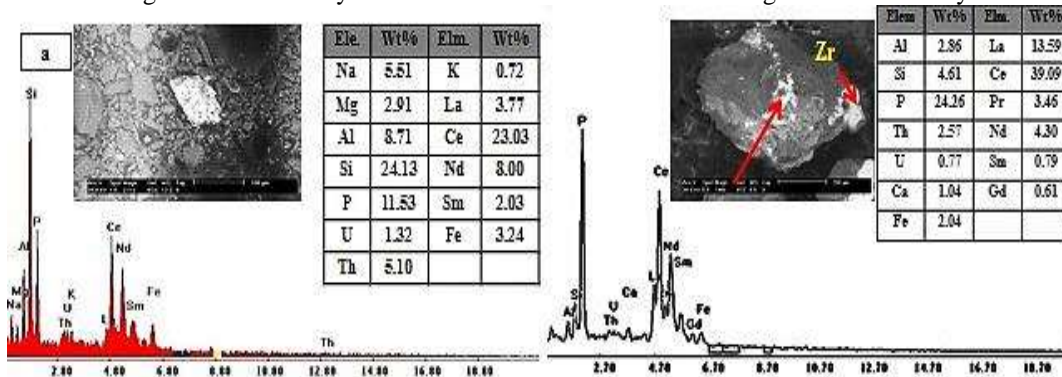


Fig. 23:BSE images and EDX analyses of a) monazite and b) Cerianite.

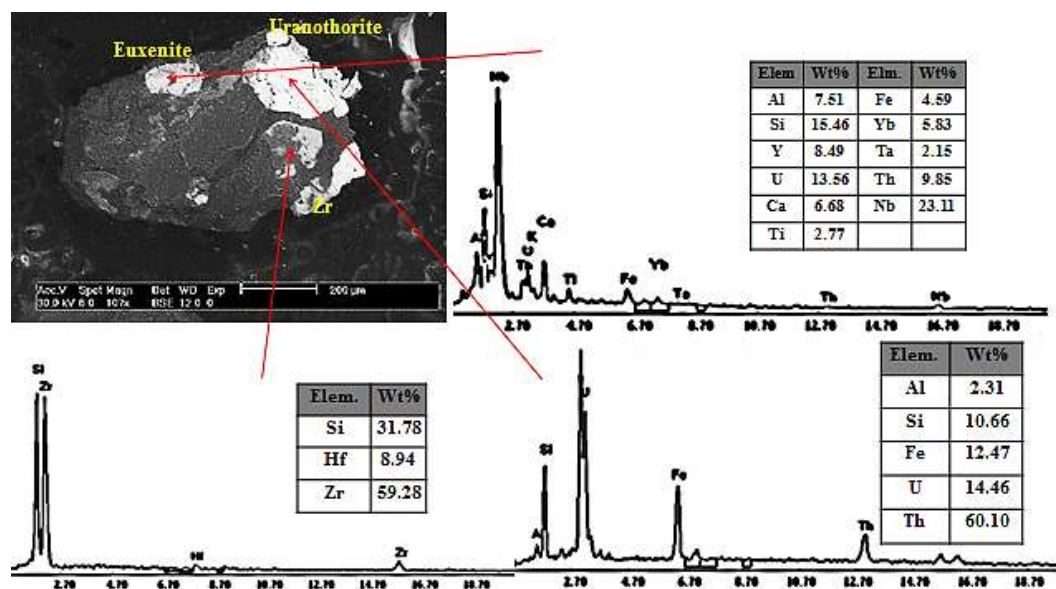


Fig. 24: BSE images and EDX analyses of composite grain contain Euxenite, uranothorite and zircon.

[29]. The mineralized microgranite's HFSE and total REE (TREE) content are unusual in less altered and normal granites. For example, the TREEs increase from 28.5 ppm to 3373.8 ppm, with more enrichment with heavy rare earth minerals relative to light rare earth minerals. In mineralized microgranite, the HFSEs increase relative to those in the less altered microgranite, especially thorium, which increases 546 fold in the former compared to its original content in the latter. The magma chamber's final magma ring at Abu Hadeidah involved the formation of microgranitic veins; a process associated with highly developed fluids rich in Na and F. These fluids caused thermo-hydrothermal changes diffused along separate fluid pathways in the dams and fine veins containing an abundance of allanite, Zircon, apatite and rare earth element content. The compound REEs were refilled with F in liquids, then re-deposited in dams and microscopic veins along weak levels, resulting in formation of the mineralized zone. The occurrence of radioelement-bearing minerals like Zircon, xenotime, thorite, uranothorite, columbite, apatite, and allanite in the studied microgranite may lead to the metamictization of minerals and a loose structure. The reaction between metamict mineral and the hydrothermal fluid leads to an alteration in the chemical composition, in which the primary substitution mechanisms are showed (Fig.24). Metamictization and hydration give lead to volume expansion and the consequent formation of cracks. These cracks indicate fluid eruption and related reaction processes. The alteration of thorite and Zircon in high- and low-temperature solutions was recorded by [28,30]. The recorded zircon granules showed a solid fraction of the complete solution with thorite and uranothorite. Euhedral fresh allanite and subhedral altered allanite are also present, as indicated by the petrological studies and EDAX analyses. Zircon and other associating minerals (like xenotime, thorite, uranothorite, apatite, allanite and others) may interact with the surrounding solutions. These solutions

become characterized with different elements (such as Zr, Hf, Th, U, Nb, Ta, Ti, and REEs) and affect pre-existing minerals to varying degrees according to mineral strength. The presence of dark, patchy areas filled with unusual minerals in metamict and cracked zircon grains, like thorite, uranothorite, and Euxenite, suggest the role of hydrothermal solutions in the redistribution of these elements and construct new miners associations such as the euxenite-polycrase series, the columbite-tantalite series, the samarskite group, uranium-thorium minerals, rare earth minerals (cerianite), Zircon and monazite.

5 Conclusions

The rock units investigated in the Southeastern part of the Wadi Baroud area can be arranged from oldest to youngest as follows; older granites, younger gabbros, younger granites, microgranites offshoots and basic and acidic dikes. This radioactive mineralization occurrence, located to the South part of Wadi Baroud, is a first for Abu Hadeida microgranite. Petrographically, Zircon, allanite, iron oxides, and opaques are the main U and rare earth minerals, while kasolite, thorite, uranophane, and curite are the predominant radioactive minerals. These rocks are considered high Uranium, high thorium rocks due to these two elements' high level. Mineralogically, the studied area is enriched with many rare accessory minerals, such as the euxenite-polycrase series, the columbite-tantalite series, the samarskite group, uranium-thorium minerals, rare earth minerals (cerianite), Zircon, and monazite. Zircon and other associating minerals (like xenotime, thorite, uranothorite, xenotime, apatite, allanite and may be other minerals) can react with surrounding solutions and could be the source of the rare radioactive metals in these rocks.

Acknowledgements: The authors would like to thank professor Mohamed Galal El Feky for collecting samples and access to the labs at Nuclear Materials Authority, Egypt.

Author contributions: All authors were responsible for writing, data collection, figure drafting, interpretation of results, editing, and supervision.

Funding This work was not funded

Compliance with ethical standards

Conflict of interest The authors declare that they have no conflict of interest.

References

- [1] J., Jacobs, R.J., Thomas, Himalayan-type indenter-escape tectonics model for the southern part of the late Neoproterozoic-early Paleozoic East African-Antarctic orogen. *Geology.*, **32**, 721–724, (2004). <https://doi.org/10.1130/G20516.1>
- [2] R.J., Stern, ARC Assembly and Continental Collision in the Neoproterozoic East African Orogen: Implications for the Consolidation of Gondwana land. *Annu. Rev. Earth Planet. Sci.*, **22**, 319–351 (1994). <https://doi.org/10.1146/annurev.earth.22.050194.001535>
- [3] A., Shalaby, K., Stüwe, F., Makroum, H., Fritz, T., Kebede, U., Klötzli, The Wadi Mubarak belt, Eastern Desert of Egypt: A Neoproterozoic conjugate shear system in the Arabian-Nubian Shield. *Precambrian Res.*, **136**, 27–50 (2005). <https://doi.org/10.1016/j.precamres.2004.09.005>
- [4] S., El-Gaby, F.K., List, R., Tehrani, Geology, evolution and metallogenesis of the Pan-African belt in Egypt, in: *The Pan-African Belt of Northeast Africa and Adjacent Areas: Tectonic Evolution and Economic Aspects of a Late Proterozoic Orogen.*, 17–68 (1988).
- [5] B.H., Ali, S.A., Wilde, M.M.A., Gabr, Granitoid evolution in Sinai, Egypt, based on precise SHRIMP U-Pb zircon geochronology. *Gondwana Res.* **15**, 38–48, (2009). <https://doi.org/10.1016/j.gr.2008.06.009>
- [6] P.R., Johnson, A., Andresen, A.S., Collins, A.R., Fowler, H., Fritz, W., Ghebreab, T., Kusky, R.J., Stern, Late Cryogenian-Ediacaran history of the Arabian-Nubian Shield: A review of depositional, plutonic, structural, and tectonic events in the closing stages of the northern East African Orogen. (2011). *J. African Earth Sci.* <https://doi.org/10.1016/j.jafrearsci.2011.07.003>
- [7] D.B., Stoesser, C.D., Frost, Nd, Pb, Sr, and O isotopic characterization of Saudi Arabian Shield terranes. *Chem. Geol.* **226**, 163–188, (2006). <https://doi.org/10.1016/j.chemgeo.2005.09.019>
- [8] I. A., Abu El-Leil, A. S., Tolba, S. A. M., Omar, M. G., El-Feky, M. H., Bakiet, H. A., Awad, Radioactive Mineralization of El-Missikat Granite; one of Most Important Occurrence, Eastern Desert, Egypt. *Int. J. Innov. Sci. Eng. Technol.*, **2**, 2348 – 7968 (2015).
- [9] A., EL Hadary, A., Soliman, A., Omran, Contributions to the Geology and Mineralogy of Wadi Ras Abda Area, North Eastern Desert, Egypt. *Nucl. Sci. Sci. J.* **4**, 47–59, (2015). <https://doi.org/10.21608/nssj.2015.30837>
- [10] A.A., Omran, Geology, Mineralogy and Radioelements Potentially of Microgranite Dike to The South Of Wadi Abu Hadeida Area, Northern Eastern Desert, Egypt. *Al-Azhar Bull. Sci.*, **25**, 47–62, (2014). <https://doi.org/10.21608/absb.2014.22610>
- [11] A.A., Omran, Geological, petrochemical studies and potentiality of uranium-thorium occurrences in Gabal Um Taghir El-Tahtani area with emphasis on the granitic rocks, Central Eastern Desert, Egypt. *Al Azhar Bulletin of Science.*, **25**, 47-62 (2005).
- [12] M., Abd El Monsif, Geochemistry and Radioactive Mineralization Inspections of the Pegmatite Bodies Associating Variable Granitic Environs, Abu Hadeida Area, North Eastern Desert, Egypt. *Journal of Basic and Environmental Sciences.*, **8**, 1-14 (2021). ISSN 2356-6388, 2536-9202.
- [13] A.H., Hussein, Lecture Course in Nuclear Geology, 101p. (1978). NMA, Egypt.
- [14] S.L., Hanson, W.B., Simmons, A.U., Falster, E.E., Foord, F.E., Lichte, Proposed nomenclature for samarskite-group minerals: new data on ishihawaite and calciosamarskite. *Mineral. Mag.*, **63**, 27–36, (1999). <https://doi.org/10.1180/002646199548286>
- [15] B.A., Simmons, F. Dobbin, G. Garrett. Introduction: the international diffusion of liberalism. *International Organization.*, **60**(4), 781-810 (2006).
- [16] E. H., Nickel J. A., Mandarino Procedures involving the IMA Commission on New Minerals and Mineral Names, and guidelines on mineral nomenclature. *Acta Petrologica et Mineralogica.*, **6**, 252–278 (1987).
- [17] T.S., Ercit, The geochemistry and crystal chemistry of columbite-group minerals from granitic pegmatites, southwestern Grenville Province, Canadian Shield. *Can. Mineral.*, **32**, 421–438 (1994).
- [18] T.S., Ercit, M.A., Wise, P., Cerny, Compositional and structural systematics of the columbite group. *Am. Mineral.*, **80**, 613–619 (1995). <https://doi.org/10.2138/am-1995-5-619>
- [19] G.H., Heinrich, Synopsis of Nearctic Ichneumoninae Stenopneusticae with particular reference to the Northeastern region (Hymenoptera). Part V. Synopsis of the Ichneumonini: Genera *Protopelmus*, *Patrocloides*, *Probolus*, *Stenichneumon*, *Aoplus*, *Limonethe*, *Hybophorellus*, *Rubic*. *Canadian Entomologist. Suppl.*, **26**, 507-672 (1962).
- [20] F., Poitrasson, J.L., Paquette, J.M., Montel, C., Pin, J.L., Duthou, Importance of late-magmatic and hydrothermal fluids on the Sm-Nd isotope mineral systematics of hypersolvus granites. *Chem. Geol.* **146**, 187–203 (1998). [https://doi.org/10.1016/S0009-2541\(98\)00010-2](https://doi.org/10.1016/S0009-2541(98)00010-2)
- [21] T.S., Ercit, Identification and alteration trends of

- granitic-pegmatite-hosted (Y,REE,U,Th)-(Nb,Ta,Ti) oxide minerals: A statistical approach. *Can. Mineral.* **43**,1291–1303, (2005).<https://doi.org/10.2113/gscanmin.43.4.1291>
- [22] R.C., Ewing, The crystal chemistry of complex niobium and tantalum oxides. IV. The metamict state: Discussion. *Am. Mineral.*, **60**, 728–733 (1975).
- [23] D.D.,Hogarth,Classification and nomenclature of the pyrochlore group. *Am. Mineral.*, **62**, 403-410 (1977).
- [24] G.R., Lumpkin, R.C., Ewing, Geochemical alteration of pyrochlore group minerals: Betafite subgroup. *American Mineralogist.*, **81**, 1237-1248 (1996).
- [25] D., Atencio, R., Gieré, M.B., Andrade, A.G., Christy, P.M., Kartashov, The pyrochlore supergroup of minerals: Nomenclature. *Can. Mineral.*, **48**, 673–678,(2010). <https://doi.org/10.3749/canmin.48.3.673>
- [26] E.J.W., Whittaker, R., Muntus, Ionic radii for use in geochemistry. *Geochim. Cosmochim. Acta.*, **34**, 945–956(1970). [https://doi.org/10.1016/0016-7037\(70\)90077-3](https://doi.org/10.1016/0016-7037(70)90077-3)
- [27] T., Akagi, A. A., Masuda, simple thermodynamic interpretation of Ce anomaly. *Geochem. J.*, **32**, 301–314(1998). <https://doi.org/10.2343/geochemj.32.301>
- [28] O.A., Ebyan, H.A., Khamis, A.R., Baghdady, M.G., El-Feky, N.S., Abed, Low-temperature alteration of uranium–thorium bearing minerals and its significance in neof ormation of radioactive minerals in stream sediments of Wadi El-Reddah, North Eastern Desert, Egypt. *Acta Geochim.*, **39**, 96–115 (2020). <https://doi.org/10.1007/s11631-019-00335-z>
- [29] A., Abdel Hamid, H.I., El Sundoly, A.A., Abu Steet, Hydrothermal alteration and evolution of Zr-Th-U-REE mineralization in the microgranite of Wadi Ras Abda, North Eastern Desert, Egypt. *Arab. J. Geosci.* **11**, 1–15(2018). <https://doi.org/10.1007/s12517-018-3623-2>
- [30] H.H., Abd El-Naby, High and low temperature alteration of uranium and thorium minerals, Um Ara granites, South Eastern Desert, Egypt. *Ore Geol. Rev.* **35**,436–446(2009). <https://doi.org/10.1016/j.oregeorev.2009.02.006>.